Acta Pharmaceutica Sinica B 2024;14(10):4608–4618

Chinese Pharmaceutical Association
Institute of Materia Medica, Chinese Academy of Medical Sciences

Acta Pharmaceutica Sinica B

www.elsevier.com/locate/apsb
www.sciencedirect.com

ORIGINAL ARTICLE

Engineering the microenvironment of P450s to enhance the production of diterpenoids in *Saccharomyces cerevisiae*

Yatian Cheng [a], Linglong Luo [a], Hao Tang [a,b], Jian Wang [a], Li Ren [a], Guanghong Cui [a], Yujun Zhao [a], Jinfu Tang [a], Ping Su [a], Yanan Wang [a], Yating Hu [c], Ying Ma [a,*], Juan Guo [a,*], Luqi Huang [a,*]

[a]*National Resource Center for Chinese Materia Medica, China Academy of Chinese Medical Science, State Key Laboratory of Dao-di Herbs, Beijing 100700, China*
[b]*School of Pharmacy, Nanjing University of Chinese Medicine, Nanjing 210023, China*
[c]*School of Traditional Chinese Medicine, Capital Medical University, Beijing 100069, China*

Received 2 March 2024; received in revised form 17 April 2024; accepted 18 May 2024

KEY WORDS

Saccharomyces cerevisiae;
Metabolic engineering;
P450s;
Tanshinones;
11,20-Dihydroxyferruginol

Abstract Cytochrome P450 enzymes play a crucial role as catalysts in the biosynthesis of numerous plant natural products (PNPs). Enhancing the catalytic activity of P450s in host microorganisms is essential for the efficient production of PNPs through synthetic biology. In this study, we engineered *Saccharomyces cerevisiae* to optimize the microenvironment for boosting the activities of P450s, including coexpression with the redox partner genes, enhancing NADPH supply, expanding the endoplasmic reticulum (ER), strengthening heme biosynthesis, and regulating iron uptake. This created a platform for the efficient production 11,20-dihydroxyferruginol, a key intermediate of the bioactive compound tanshinones. The yield was enhanced by 42.1-fold through 24 effective genetic edits. The optimized strain produced up to 67.69 ± 1.33 mg/L 11,20-dihydroxyferruginol in shake flasks. Our work represents a promising advancement toward constructing yeast cell factories containing P450s and paves the way for microbial biosynthesis of tanshinones in the future.

*Corresponding authors.
E-mail addresses: xiaoma1110@126.com (Ying Ma), guojuanzy@163.com (Juan Guo), huangluqi01@126.com (Luqi Huang).

Peer review under the responsibility of Chinese Pharmaceutical Association and Institute of Materia Medica, Chinese Academy of Medical Sciences.

https://doi.org/10.1016/j.apsb.2024.05.019

1. Introduction

Cytochrome P450 (P450) enzymes were initially identified in the early 1960s and constitute one of the largest and most diverse protein superfamilies known, present widely across various life kingdoms[1-3]. The indispensable roles of P450s in mammalian drug metabolism underscore their significant implications in medicine and pharmacology[4,5]. In plants, the rapidly expanding P450 family serves as versatile oxidase biocatalysts in the synthesis of diverse natural products[6,7]. For instance, P450s are involved in more than 97% of diterpene biosynthesis[8,9]. Multiple P450s participate in various pathways for the synthesis of pharmacologically active PNPs[10], such as paclitaxel, a key anti-cancer ingredient, involving eight P450s (*T5αH*, *T10βH*, *T2αH*, *T7βH*, *T13αH*, *T2′αH*, *TOT*, and *T9αH*)[11]. Notably, the pharmacological activities of many PNPs are mediated by their complex oxidative groups, which are formed by P450s, such as alkaloids[12], isoflavonoids[13], and terpenoids[14-16]. However, heterologous expression of plant P450s often results in poor chemical and regional selectivity in microbial hosts, hampering the bioproduction of PNPs. Furthermore, P450-mediated catalytic reactions in microbial hosts frequently serve as the rate-limiting steps in PNP biosynthesis, constraining product yields in microbial cell factories. Thus, enhancing the expression level and catalytic performance of P450s is imperative for increasing PNP production in microbial hosts.

The reaction catalyzed by P450s typically involves a mixed-function oxidase process comprising several components, such as heme-thiolate-containing enzymes P450s, cofactors (reduced nicotinamide adenine dinucleotide phosphate, NADPH), and redox partners (such as cytochrome P450 reductase, CPR), which act as electron transfer shuttles[17]. To harness the catalytic potential of P450s, scientists have explored various strategies for their functional expression in the preferred chassis *S. cerevisiae*. These strategies include protein engineering, codon optimization, metabolic engineering to enhance NADPH supply, expand the ER, strengthen heme biosynthesis in *S. cerevisiae*, and so on (Fig. 1). Additionally, CPRs harbor two flavin domains, flavin-adenine dinucleotide (FAD) and flavin mononucleotide (FMN)[18]. However, the potential of metabolic engineering targeting the FAD(H_2) pathway to enhance CPR activity in yeast remains unexplored. Moreover, iron is an important component of P450s and an essential factor in various oxidation−reduction reactions in yeast. However, there is currently limited research on the effect of iron regulation on improving P450 catalytic activity, which deserves further investigation. Based on these studies and regulatory strategies that need to be validated, we combined multiple strategies to comprehensively modify the expression environment of P450s in yeast to ensure the efficient expression and continuous catalysis of multiple exogenous P450 proteins.

Tanshinones, the principal bioactive diterpenoid constituents found in *Salvia miltiorrhiza* Bunge, exhibit notable pharmacological properties, including cardiovascular effects and antitumor activities[21]. The biosynthesis of tanshinones involves a series of enzymatic reactions, with P450 enzymes playing a crucial role in modifying the characteristic phthaloquinone structure of these compounds. Geranylgeranyl diphosphate (GGPP), serving as the common precursor of diterpenoids, initiates the biosynthetic pathway of tanshinones[22]. Specifically, GGPP is catalyzed by bycopalyl diphosphate synthase (SmCPS1) and kaurene synthase-like (SmKSL1) from *S. miltiorrhiza* Bunge to form miltiradiene, a crucial intermediate in tanshinone biosynthesis[23]. Then, three P450s SmCYP76AH1, SmCYP76AH3, and SmCYP76AK1 from *S. miltiorrhiza* Bunge catalyze hydroxylation at carbon-12 (C12), C11, and C20, yielding 11,20-dihydroxyferruginol[24,25] (Fig. 2). The catalytic versatility of P450 enzymes results in the formation of a complex network of tanshinone biosynthesis, generating various intermediate products. 11,20-Dihydroxyferruginol has been identified as a pivotal intermediate in the biosynthetic pathway of tanshinones, and is further processed into tanshinones through the various enzymes including P450s[23,24]. In recent decades, significant efforts have been directed toward the efficient production of tanshinone precursors in engineered yeast. Zhou et al. successfully employed a modular pathway engineering strategy to enhance miltiradiene production, achieving a titer of 365 mg/L in a 15-L bioreactor culture[26]. Similarly, Hu et al. engineered a high-yield GGPP chassis strain and identified diterpene synthases with optimal efficiency, notably truncated SmKSL1 (tSmKSL1) protein fused with diterpene synthase CfTPS1 from *Coleus forskohlii*, resulting in a final yield of 550.7 mg/L miltiradiene in shake flasks[27]. However, incorporating the first P450 module (*SmCYP76AH1* coexpressed with *SmCPR1*) into the aforementioned miltiradiene chassis led to the heterologous production of ferruginol at 10.5 mg/L[25]. The subsequent introduction of the second P450 module (the *SmCYP76AH3* and *SmCYP76AK1* assembly module) resulted in the simultaneous expression of three P450s in the engineered yeast, leading to a decreased yield of 11,20-dihydroxyferruginol to 1.2 mg/L[24]. This significant reduction in end products indicated inefficient utilization of substrates by the P450 enzymes, thereby limiting the metabolic flow of the tanshinone biosynthetic pathway. Consequently, optimizing the catalytic environment and efficiency of P450 enzymes in yeast is crucial and challenging for the bioproduction of tanshinones.

In this study, we aimed to engineer *S. cerevisiae* to create an optimal microenvironment for three P450s in the biosynthesis of the tanshinone precursor 11,20-dihydroxyferruginol. Our approaches included several strategies: strengthening the MVA pathway, co-expressing with redox partner genes, integrating *TRP1*, *LYS2* and

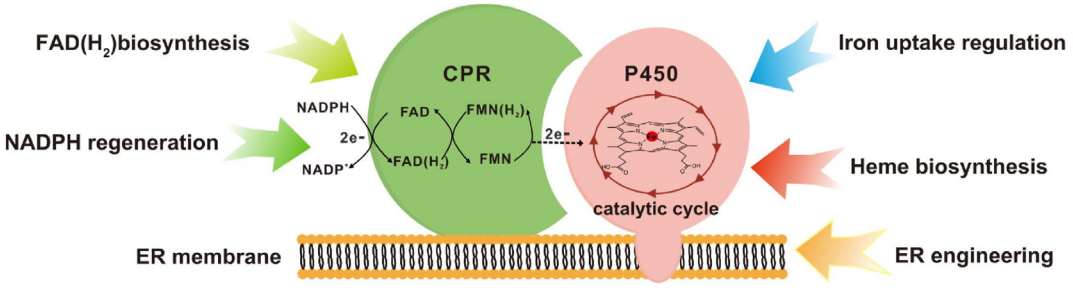

Figure 1 Schematic representation of the metabolic engineering strategies of plant P450 and CPR in yeast[19,20].

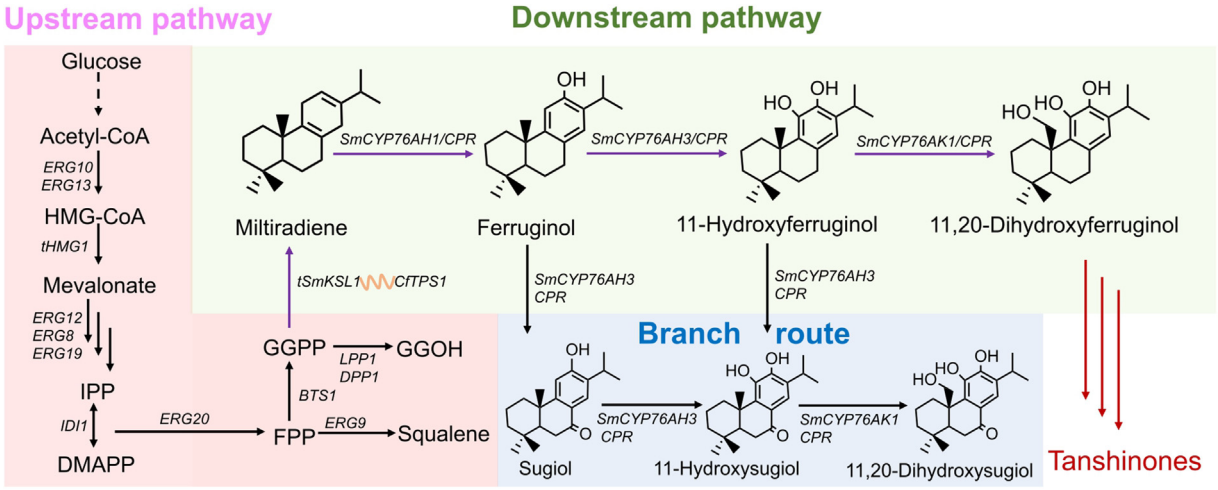

Figure 2 Biosynthesis of 11,20-dihydroxyferruginol in *S. cerevisiae*. FPP: farnesyl pyrophosphate, GGOH: geranylgeraniol, acetyl-CoA: acetyl-coenzyme A, HMG-CoA: hydroxymethylglutaryl-coenzyme A, *ERG10*: acetoacetyl-CoA thiolase gene, *ERG13*: genehydroxymethylglutaryl-CoA synthase gene, *tHMG1*: truncated hydroxymethylglutaryl-CoA reductase 1 gene, *ERG12*: mevalonate kinase gene, *ERG8*: phosphomevalonate kinase gene, *ERG19*: mevalonate pyrophosphate decarboxylase gene, *IDI1*: isopentenyl diphosphate isomerase gene, *ERG9*: squalene synthase gene, *ERG20*: farnesyl diphosphate synthase gene, *LPP1*: lipid phosphate phosphatase gene, *DPP1*: bifunctional diacylglycerol diphosphate phosphatase/phosphatidate phosphatase gene, *BTS1*:geranylgeranyl diphosphate synthase gene. The curve represents the peptide linker GGGS and the dotted line represents multistep reactions.

LEU2 genes, enhancing the supply of NADPH and heme, expanding the ER, and regulating iron uptake. The expression efficiency of P450s was evaluated by the yield of 11,20-dihydroxyferruginol. Through the systematic integration of these strategies to optimize the overall catalytic microenvironment of P450s in yeast, we achieved a remarkable 42.1-fold increase in 11,20-dihydroxyferruginol production. Our research indicated that regulating the metabolic flow of iron significantly enhanced the catalytic activity of P450s, providing valuable insights into the mechanism underlying the interaction between iron uptake and the catalytic activity of P450s.

2. Materials and methods

2.1. Strains, plasmids and reagents

The *S. cerevisiae* strain BYHZ16 (*MATα*, *LEU2Δ0*, *LYS2Δ0*, *MET15*, *URA3Δ0*, *TRP1Δ::HIS3-PGK1p-BTS1/ERG20-ADH1t-TDH3p-SaGGPS-TPI1t-TEF1p-tHMG1-CYC1t*, *ROX1Δ*, *ERG9Δ218-175*, *YJL064wΔ*, and *YPL062wΔ*) used as the background strain for strain construction in this study and the p426-URA3-gRNA plasmid[27] were obtained from Professor Wei Gao. Both pECAS9-gRNA-KanMX-tHFD1[28] and pgRNA-KanMX were kind gifts from Professor Yongjin Zhou. *Escherichia coli DH5α* was used for plasmid construction and amplification. The plasmids and strains utilized in this study were listed in Supporting Information Tables S1 and S2, respectively. Kod One Master Mix was purchased from TOYOBO (Beijing, China). High-fidelity PrimeStar DNA polymerase was purchased from TaKaRa (Beijing, China) and used for routine DNA fragment amplification. PrimeSTAR Max premix (2×) and PrimeStar DNA polymerase for *in vitro* fusion PCR and T4-ligase kits used for gRNA plasmid construction were purchased from TaKaRa (Beijing, China). YeaStarTM genomic DNA kits were purchased from Zymo Research (Beijing, China). Total RNA from *S. miltiorrhiza* Bunge was extracted using a Total RNA Kit (TIANGEN, China). The total RNA above was then reverse-transcribed into cDNA using Superscript™ IV according to the manufacturer's protocol (Invitrogen, USA). DNA gel purification and plasmid extraction kits were purchased from TransGen Biotech (Beijing, China).

The codon-optimized *tSmKSL1*, *CfTPS1*, *Bacillus subtilis BsRIBBA* and *Thermotoga maritima TmBiFADS* genes were chemically synthesized by GenScript (Nanjing, China). Other foreign genes used in this study are preserved in our laboratory-and listed in Supporting Information Table S3. Sterile 50% (*w/v*) PEG3350, glucose and lithium acetate were purchased from Yuanye Biotech (Shanghai, China). 11,20-Dihydroxyferruginol was synthesized according to a previously reported method[29]. Sugiol, ferruginol, GGOH, and hemin were purchased from Yuanye Biotech (Shanghai, China). Riboflavin was obtained from Sigma−Aldrich (Beijing, China). Miltiradiene and 11-hydroxysugiol were separated from strains YT004 and YT016 by removing the *SmCYP76AK1* gene, respectively. Synthetic complete medium without uracil (SC-URA) and SC medium were purchased from FunGenome (Beijing, China). G418 was purchased from Sangon Biotech (Beijing China). Other chemicals, including analytical standards, were procured from Yuanye Biotech (Shanghai, China) unless otherwise specified.

2.2. Genetic manipulation

For gene overexpression and deletion, donor DNA fragments were assembled *in vitro* and integrated at target genomic loci using the CRISPR/Cas9 system[30]. Specific chromosomal loci (Supporting Information Table S4) were chosen for the expression of heterologous genes, resulting in stable and high-level gene expression[31-33]. The downstream pathway biosynthetic genes were transcriptionally controlled by strong galactose regulatory (GAL) promoters (*GALps*). And other overexpressed genes, including CPRs, were operated by strong constitutive promoters. The donor DNA fragments were assembled *in vitro via* an overlapping extension PCR procedure[26]. The genomic DNA of strains BY4741 and BYHZ16 was extracted with a YeaStar genomic DNA kit and served as a template for the amplification of native promoters, genes and terminators.

The specific target 20 bp sequences of the genomic loci were designed with the CHOPCHOP webtool (http://chopchop.cbu.uib.no) for gRNA plasmid construction. The p426-URA3-gRNA plasmid was digested by *AarI* (NEB, Beijing, China) to obtain a linear double−strand DNA skeleton and then recombined with specific target 20 bp sequences that contained 4 bp DNA sequence parts of gRNA *in vitro*. All primers used to construct the donor DNA fragments, PCR identification and gRNA vectors were synthesized by Sangon Biotech (Beijing, China) and are listed in Supporting Informations Tables S5−S7, respectively.

The optimized lithium acetate-mediated yeast transformation protocol[34] was used in this study (Supporting Information Table S8). SC-URA, with 20 g/L glucose and 20 g/L agar, was used for the selection of yeast transformants for selecting correct colonies. Yeast colonies with genetic modifications were verified by colony PCR using Kod One Master Mix to identify correct transformants. Partial colonies of correct transformants were transferred to 20 μL of 20 mmol/L NaOH, boiled for 20 min at 99 °C, and centrifuged for 2 min, after which 2 μL of each supernatant was used as a template for yeast colony PCR. Then, the remaining correct colonies were scribed on SC supplemented with 1 g/L 5-fluoroorotic acid (5-FOA, Sigma−Aldrich, Beijing, China) plates and cultured at 30 °C to remove the p426-URA3-gRNA plasmid.

2.3. Strain fermentation in shake flasks

YPD medium, consisting of 20 g/L peptone (OXOID, Beijing, China), 10 g/L yeast extract (OXOID, Beijing, China), and 20 g/L glucose was used for yeast cultivation and preparation of competent cells. The defined minimal medium contained 7.5 g/L $(NH_4)_2SO_4$, 14.4 g/L KH_2PO_4, 0.5 g/L $MgSO_4 \cdot 7H_2O$, 20 g/L glucose, 2 mL of trace metal solution, and 1 mL of vitamin solution, which were prepared according to a reported procedure[13].

For shake flask batch fermentations, YPD medium supplemented with 20 g/L glucose and 10 or 20 g/L galactose was used to induce the transcription of genes under the control of *GALps*. A defined minimal medium was also utilized for shake flask batch fermentation. When required, the minimal medium was supplemented with 60 mg/L of uracil or other amino acids. The strains were seeded into the medium to an initial OD_{600} (optical density at 600 nm) of 0.2 measured with a UV spectrophotometer (Meixi, Shanghai) in this study. Shake flask batch fermentations were cultured at 30 °C with 200 rpm agitation. The biomass of engineered *S. cerevisiae* was monitored by OD_{600} at the end of fermentation. A flowchart of the construction of all strains used in this study was shown in Supporting Information Fig. S1.

2.4. Product extraction, analysis and quantification

For the extraction of GGOH, miltiradiene and ferruginol, 0.5 mL of culture broth from shake flask batch fermentation was added to an equal volume of *n*-hexane, vortexed thoroughly for 5 min, and centrifuged at 13,000 × rpm for 12 min. The *n*-hexane phase was collected and diluted in an equal volume of *n*-hexane for analysis by gas chromatography-mass spectrometry (GC−MS, Thermo Fisher Scientific, USA) equipped with a TR-5 ms capillary column (30 mm × 0.25 mm i.d., 0.25 μm film thickness, Thermo Fisher Scientific, USA). The parameters used for GC−MS analysis was described in Supporting Information Table S9. For the extraction of 11,20-dihydroxyferruginol and other products, 0.5 mL of culture broth were added to an equal volume of ethyl acetate, vortexed thoroughly for 5 min, and centrifuged at 13,000 × rpm for 5 min, after which 0.3 mL of the ethyl acetate phase were collected, dried, and resuspended in methanol and centrifuged at 13,000 × rpm for 12 min for UPLC or LC−MS analysis. The products were quantified on an ultimate high-performance liquid chromatograph (UPLC, Waters, Germany) equipped with a BEH 5 cm × 2.1 mm column (particle size 1.7 μm, Waters, Germany) connected to a photodiode array (PDA) detector (280 nm). An Agilent Eclipse Plus C18 column (RRHD 1.8 μm, 2.1 mm × 100 mm) was used for LC coupled to quadrupole time-of-flight MS (LC−QTOF-MS, Agilent Technologies, USA) in negative ion mode to detect products. The parameters for metabolites quantification by UPLC and LC−MS/MS are shown in Supporting Information Table S10. Standard deviations were calculated from three biologically independent samples using GraphPad Prism version 9.4.0 (GraphPad Software, USA). The statistical significance was determined *via* *t*−tests (*$P < 0.05$, **$P < 0.01$, ***$P < 0.001$ and ****$P < 0.0001$, ns, not significant). The standard curves of metabolites are shown in Supporting Information Fig. S2.

2.5. Quantification of the NADPH/$NADP^+$ ratio, heme and riboflavin contents in yeast

$NADP^+$ and NADPH assays were performed using a CheKine $NADP^+$/NADPH assay kit (catalog no. WST-8, Abbkine, Wuhan, China). For the extraction of riboflavin, 0.5 mL of culture broth from shake flask batch fermentation was centrifuged at 13,000 × rpm for 5 min, and the yeast cells and supernatant were isolated. The supernatant was transferred to a new tube, added to an equal volume of methanol, and vortexed thoroughly for 5 min for analysis of extracellular riboflavin. Then, 0.5 mL of methanol was added to the isolated yeast cells, which were then subjected to bead-heating for 8 min at 60 Hz (broken for 1 min and paused for 1 min for a total of 8 min) for analysis of intracellular riboflavin. The extract solution was filtered through a 0.22 μm organic membrane before UPLC analysis. The method of analyzing riboflavin was designed and performed according to the procedure described in Ref. 35 (Supporting Information Table S11). The intracellular heme concentration was measured by oxalic acid treatment as described in previous reports[36,37]. The fluorescence was detected on a Varioskan LUX plate reader spectrophotometer (Thermo Fisher Scientific, USA).

3. Results and discussion

3.1. Modular construction of the 11,20-dihydroxyferruginol biosynthetic pathway in S. cerevisiae

BYHZ16 is a genetically modified yeast strain capable of biosynthesizing the diterpenoid precursor GGPP[27]. To establish a robust platform for multi-gene manipulation, *SpCas9* and *KanMX* gene cassettes were integrated into the genomic *XI-5*[31] locus in strain BYHZ16. Subsequently, we used a guide RNA (gRNA) targeting the *KanMX* marker gene to excise it[38], resulting in the generation of strain BYHZ16::Cas9. This strain served as our foundational chassis for subsequent engineering endeavors. In the engineered strain BYHZ16::Cas9, we established the biosynthetic pathway for miltiradiene production, serving as the pivotal precursor for 11,20-dihydroxyferruginol (Fig. 3A). One and two copies of codon-optimized *tSmKSL1* and *CfTPS1* fusion genes, driven by the strong promoter *GAL10p*, were integrated into two

diffferent genomic loci resulted in YT001 and YT002, respectively. Product analysis revealed that strain YT002 yielded 19.93 ± 4.22 mg/L of miltiradiene in the YPD medium supplemented with 20 g/L of galactose, which was 2.6 times higher than strain YT001 (Fig. 3B). To further enhance miltiradiene production, one additional copy of the *tSmKSL1* and *CfTPS1* fusion genes were overexpressed, and the galactose-utilizing *GAL1/10/7* genes were knocked out in strain YT002, resulting in strain YT004. The results demonstrated that the miltiradiene titer in strain YT004 was increased to 31.88 ± 0.53 mg/L in the YPD medium supplemented with galactose (Fig. 3B).

To construct a basal strain, we established the downstream pathway comprising P450s and CPRs within the miltiradiene chassis YT004. Strong promoters *GAL2p* and *GAL7p* were employed to drive the expression of *SmCYP76AH1*, *SmCYP76AH3* and *SmCYP76AK1* genes in yeast. Integration of a single copy of these three genes and *SmCPR1* at different genomic loci[39] in strain YT004 resulted in a 1.57 ± 0.48 mg/L production of 11,20-dihydroxyferruginol, 4.16 ± 2.03 mg/L of miltiradiene, and 8.32 ± 4.01 mg/L of ferruginol in strain YT009 (Fig. 3C and Supporting Information Fig. S3). In addition, *AtCPR1* from *Arabidopsis thaliana* has been reported to be compatible with many P450s[14]. A copy of *AtCPR1* was overexpressed in strain YT009 to generate strain YT010. YT010 strain exhibited an 81% increase compared to that of control strain YT009, which produced 2.84 ± 0.19 mg/L of 11,20-dihydroxyferruginol (Fig. 3C). The yield of products demonstrates a close correlation with the number of gene copies, highlighting the potency of overexpressing multiple gene copies as a strategy for enhancing the product yields. Due to the accumulation of ferrugiol in strain YT010 (23.39 ± 3.11 mg/L, Fig. S3), an additional copy of *SmCYP76AH3* and *SmCYP76AK1* were integrated into the genomic *YPRCδ15* locus in strain YT010. This adjustment led to a slight increase in the titer of 11,20-dihydroxyferruginol to 3.24 ± 0.50 mg/L (strain YT011, Fig. 3C). This strain was used as the base strain for 11,20-dihydroxyferruginol production for pathway optimization.

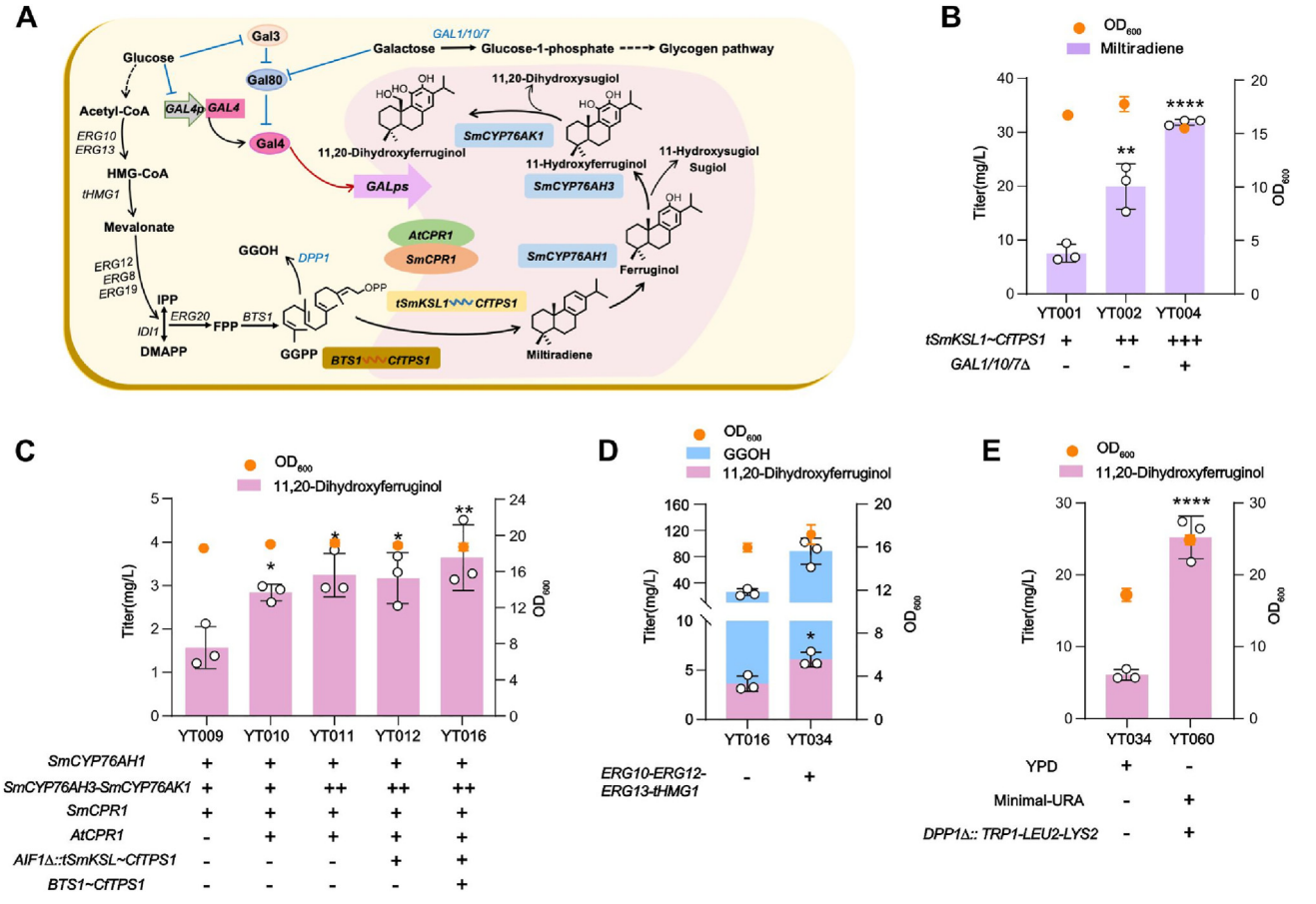

Figure 3 Modular construction of the 11,20-dihydroxyferruginol biosynthetic pathway in *S. cerevisiae*. (A) Overview of the engineered metabolic pathway for the biosynthesis of 11,20-dihydroxyferruginol in *S. cerevisiae*. The blue characters indicate genes with deletions. The blue lines represent negative regulation, and the red lines represent positive regulation. The dotted line represents multistep reactions. It includes the overexpression of key genes and *GALp*-mediated (*GAL10p*, *GAL2p/7p*) genes. *GAL4*: galactose-responsive transcription factor, *GAL3*: transcriptional regulator, *GAL1/10/7*: galactose utilizing genes. ~: linker GGGS. (B) Optimized gene dosages of the *tSmKSL1*~*CfTPS1* and knockout *GAL1/10/7* genes to construct the miltiradiene chassis. (C) The titers of 11,20-dihydroxyferruginol were measured after the overexpression of three P450s, two CPRs and the *BTS1*~*CfTPS1* fusion genes in engineered strains. (D) The titers of GGOH and 11,20-dihydroxyferruginol after overexpressing the MVA pathway genes in engineered yeast. (E) Effects of the overexpression of *TRP1*, *LEU2*, *LYS2* and deletion of *DPP1* gene on the titer of 11,20-dihydroxyferruginol. The OD_{600} was measured at the end of fermentation.

Adequate precursor supply is a prerequisite for downstream modification. We first focused on the upstream biosynthetic pathway to increase the synthesis of the precursors, including GGPP and miltiradiene. Apoptosis-inducing factor (*AIF1*) reportedly mediates chemical-induced apoptosis in *S. cerevisiae*[40,41], and deletion of *AIF1* might weaken this apoptosis. One copy of the *tSmKSL1* and *CfTPS1* fusion genes was overexpressed and *AIF1* was deleted in strain YT011, However, this modification didn't enhance the yield of 11,20-dihydroxyferruginol, as evidenced by the comparable titer observed in strain YT012 (3.17 ± 0.58 mg/L) (Fig. 3C and Supporting Information Fig. S4). The fusion of *GGPPS* and *TPS* genes has been reported to improve the flux from DMAPP to the initial diterpene diphosphate product[42]. *BTS1* and *CfTPS1* fusion genes were then overexpressed in the strain YT012. This led to a further 15% improvement (3.64 ± 0.76 mg/L, Fig. 3C) on 11,20-dihydroxyferruginol production in strain YT016 compared to that of strain YT012. For enhancing GGPP supply, four key genes (*ERG10*, *ERG13*, *tHMG1*, and *ERG12*) from the MVA pathway were overexpressed, which resulted in strain YT034. The overexpression of these genes resulted in a notable increase of 11,20-dihydroxyferruginol production, yielding a higher titer of 6.09 ± 0.96 mg/L in strain YT034 (Fig. 3D). Notably, the titer of GGOH and miltiradiene in strain YT034 was significantly improved compared to that of strain YT016 (Fig. 3D and Supporting Information Figs. S3 and S5).

To reduce fermentation costs and improve the strain growth in amino acid autotrophic status, *TRP1*, *LEU2* and *LYS2* genes were overexpressed and *DPP1* was knocked out to decrease GGOH competing for GGPP precursor in strain YT034, which resulted in strain YT060. 11,20-Dihydroxyferruginol production of strain YT060 was significantly increased to 25.22 ± 2.98 mg/L in minimal medium, representing a 314% improvement compared with that of strain YT034 in YPD medium (Fig. 3E). Strain YT060 was used as a chassis for optimizing microenvironment for P450s.

3.2. *Enhancing electron transfer and cofactor supply in the P450 electronic cycle system in yeast*

P450 requires electron transfer, and we aimed to enhance its electron transfer efficiency from two aspects, the electron transfer proteins FDR (ferredoxin reductase) and FDX (ferredoxin) and cofactors. FDXs constitute a large family of iron-sulfur proteins that shuttle electrons from FDRs into diverse biological processes[43]. To test the function of FDR and FDX involving in electrons transfer, we introduced *SmFDR* and *SmFDX* from *S. miltiorrhiza* Bunge into the yeast strain harboring the three P450s while without *CPR*, and *SmCPR1* was used as a positive control to evaluate the electron transfer efficiency. The data showed that compared with the strain harboring *SmCPR1*, the *SmFDR* and *SmFDX* overexpressed strain produced extremely low levels of 11,20-dihydroxyferruginol (Supporting Information Fig. S6). Based on this, *SmFDR* and *SmFDX* were overexpressed in strain YT060 resulting in strain YT067. However, there was no significant difference between strain YT060 and strain YT067 (Fig. 4A). Furthermore, to reduce the fermentation cost, *GAL80* was knocked out in strain YT067, resulting in strain YT071. The yield of 11,20-dihydroyferruginol was 22.69 ± 1.85 mg/L of strain YT071 without galactose in minimal medium (Fig. 4A).

NADPH is an important cofactor for P450s. Improving NADPH regeneration is anticipated to be advantageous for the biosynthesis of PNPs in which P450s are involved[13,44,45]. Overexpression of *ZWF1* and the phosphofructokinase (PFK) mutant genes $PFK1^{S724D}$ and $PFK2^{S718D}$ had been shown to decrease upper glycolytic metabolic flux and increase the supply of NADPH in *S. cerevisiae*[46] (Fig. 4B). To improve the supply of NADPH in strain YT071, we overexpressed *ZWF1* by replacing its promoter with the strong constitutive promoter *PGK1p*, and overexpressed the mutants $PFK1^{S724D}$ and $PFK2^{S718D}$ (Supporting Information Fig. S7). After engineering, it was found that the intracellular NADPH/$NADP^+$ ratio was increased by 13% in engineered strain YT080 compared to parent strain YT071 (Fig. 4C). Strain YT080 produced 29.43 ± 3.01 mg/L of 11,20-dihydroxyferruginol, which was increased by 30% (Fig. 4D and Supporting Information Fig. S8).

CPRs play a crucial role in shuttling electrons from NADPH through the FAD and FMN cofactors into the central heme group of P450s[18]. In this study, we aimed to enhance $FAD(H_2)$ biosynthesis to improve the activity of CPRs, thereby increasing the productivity of PNPs in yeast. *RIB1* and *FLX1* involved native $FAD(H_2)$ biosynthesis, *BsRIBBA* and *TmBiFADS* involved in bacterial $FAD(H_2)$ biosynthesis, and native *MCH5* importing riboflavin from extracellular into intracellular were overexpressed to strengthen the metabolic flux of $FAD(H_2)$[32] (Fig. 4B). Then, riboflavin kinase *FMN1* and the FAD synthetase gene *FAD1* were overexpressed in strain YT081 to drive metabolic flux to $FAD(H_2)$ biosynthesis. However, the $FAD(H_2)$-targeting modification exhibited no beneficial effects on 11,20-dihydroxyferruginol production (strains YT077, YT079 and YT081, Fig. 4E). We found that most of the riboflavin was excreted outside the cell, which might be the reason for the lack of increase in 11,20-dihydroxyferruginol production (Supporting Information Figs. S9 and S10). Thus, this modification was given up in the next microenvironment engineering for P450s.

3.3. *Engineering ER and increasing heme biosynthesis for the improvement of the P450 catalytic environment*

Most eukaryotic P450s are ER-localized proteins, and studies have shown that ER expansion facilitates the functional expression of membrane-localized proteins in *S. cerevisiae*[13,47]. The phospholipid biosynthesis regulatory factors *INO2* and *OPI1* have been proven to regulate the size of the ER, thereby affecting the localization and expression of membrane-localized proteins such as P450s[47,48]. We engineered *S. cerevisiae* to expand the ER by overexpressing *INO2*, deleting *OPI1* and *PAH1* encoding phosphatidate phosphatase which was supposed to compete with the precursor phospholipid in ER membrane synthesis[49] (Fig. 5A). Results have shown that the deletion of *OPI1* led to a higher 11,20-dihydroxyferruginol production of 36.40 ± 2.09 mg/L in strain YT086. However, compared with the control strain YT080, overexpression of *INO2* and deletion of *PAH1* had no or negative effects on 11,20-dihydroxyferruginol titer (Fig. 5B). Finally, to evaluate the overexpression of *INO2* and deletion of *OPI1*, overexpressing *INO2* in strain YT086 to construct strain YT097. The strain YT097 produced 39.12 ± 3.35 mg/L of 11,20-dihydroxyferruginol, resulting in a 25% improvement over strain YT080 and a slight increase compared to parent strain YT086.

The overexpression of rate-limiting enzymes within the endogenous heme biosynthetic pathway has been shown to promote heme synthesis[37] and provide more heme for the formation of active center of P450s. And it may also alleviate the pressure caused by excessive exogenous P450 expression[36]. In this study,

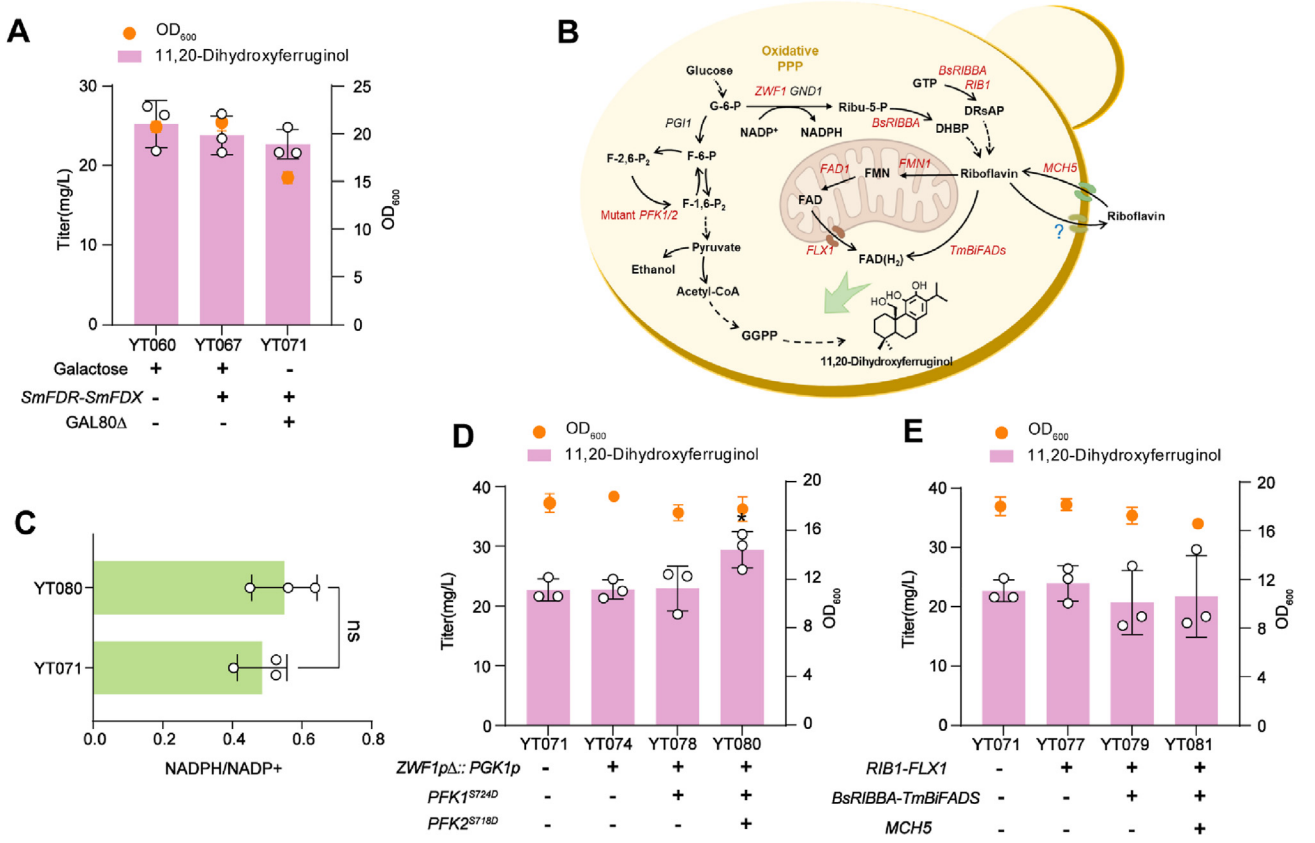

Figure 4 The effect of improving the supply of the cofactors NADPH and FAD (H_2) on the catalytic activity of P450s. (A) The 11,20-dihydroxyferruginol production by overexpression *SmFDR* and *SmFDX* and deletion of *GAL80*. (B) Schematic illustration of engineering NADPH and FAD(H_2) in yeast. Riu-5-P: ribulose 5-phosphate, G-6-P: glucose-6-phosphate, F-2,6-P_2: fructose-2,6-bisphosphate, F-1,6-P_2: fructose-1,6-bisphosphate, F-6-P: fructose-6-phosphate, *PGI1*: glucose-6-phosphate isomerase, *GND1:* phosphogluconate dehydrogenase gene, *ZWF1*: glucose-6-phosphate dehydrogenase gene, GTP: guanosine triphosphate, DHBP: 3,4-dihydroxy-2-butanone-4-phosphate, DRsAP: 2,5-diamino-6-ribosylamino-4(3*H*)-pyrimidinone 5′-phosphate, *FLX1*: mitochondrial FAD exporter gene, *RIB1*: GTP cyclohydrolase II gene, *BsRIBBA*: bifunctional DHBP synthase/GTP cyclohydrolase II gene, *TmBiFADS*: bifunctional riboflavin kinase/FAD synthase gene, *MCH5*: riboflavin transporter gene, *FMN1*:riboflavin kinase gene, *FAD1*: FAD synthetase gene. (C) The intracellular NADPH/$NADP^+$ ratio in strains YT071 and YT080. (D) 11,20-Dihydroxyferruginol production by engineering NADPH generation. (E) The titer of 11,20-dihydroxyferruginol by engineering FAD(H_2) pathway. The OD_{600} was measured at the end of fermentation.

we selected several key genes involved in heme biosynthesis to improve the intracellular content of heme (Fig. 5C). First, we overexpressed the rate-limiting gene *HEM13*, deleted heme degradation gene *HMX1*, and knocked out heme precursor glycine utilizing gene *SHM1* (encoding mitochondrial serine hydroxyl methyltransferase) in strain YT080, respectively. The overexpression of *HEM13* resulted in a slight enhancement, increasing the production of 11,20-dihydroxyferruginol to 34.71 ± 4.08 mg/L in stain YT089 (Fig. 5D). However, when *HMX1* and *SHM1* were deleted, the titer of 11,20-dihydroxyferruginol was decreased (Fig. 5D). We also tested several key target genes to regulate heme biosynthesis in strain YT089 (Supporting Information Fig. S11). However, there was no or even a slight decrease in the titer of 11,20-dihydroxyferruginol in the resultant strain (Fig. S11). The heme content was quantified in these strains (Supporting Information Fig. S12). The results indicated that the titer of 11,20-dihydroxyferruginol did not show a simultaneous increase with the heme content. It suggested that these might be related to metabolic flux balance that required further investigation. Finally, overexpressing *HEM13* in the previous ER modified strain YT097 to construct strain YT107. This resulted in a slight increase in the 11,20-dihydroxyferruginol titer of 41.49 ± 5.41 mg/L (Fig. 5E).

3.4. *Improving the production of 11,20-dihydroxyferruginol by engineering iron uptake and the iron-sulfur cluster biosynthetic pathway*

Iron-sulfur clusters serve as the active centers of FDXs which are responsible for transferring electrons to several P450s during catalytic reactions[43]. In yeast, there are two different iron-sulfur cluster (ISC) biogenesis machineries, the mitochondrial ISC biogenesis machinery and the cytosolic iron-sulfur cluster assembly (CIA) machinery[50]. Iron-sulfur cluster biosynthesis has been shown to improve the enzymatic activity of iron-sulfur enzymes[50], such as *XylD*[51]. Iron plays a pivotal role as a micronutrient in both iron-sulfur cluster and heme biosynthesis, as well as in other functional processes[52]. In yeast, iron uptake is tightly regulated by the transcriptional control of iron acquisition systems, predominantly orchestrated by iron-responsive transcription factors Aft1/2p and Yap5p, along with a siderophore-mediated iron acquisition system[53]. Under iron-replete conditions, the

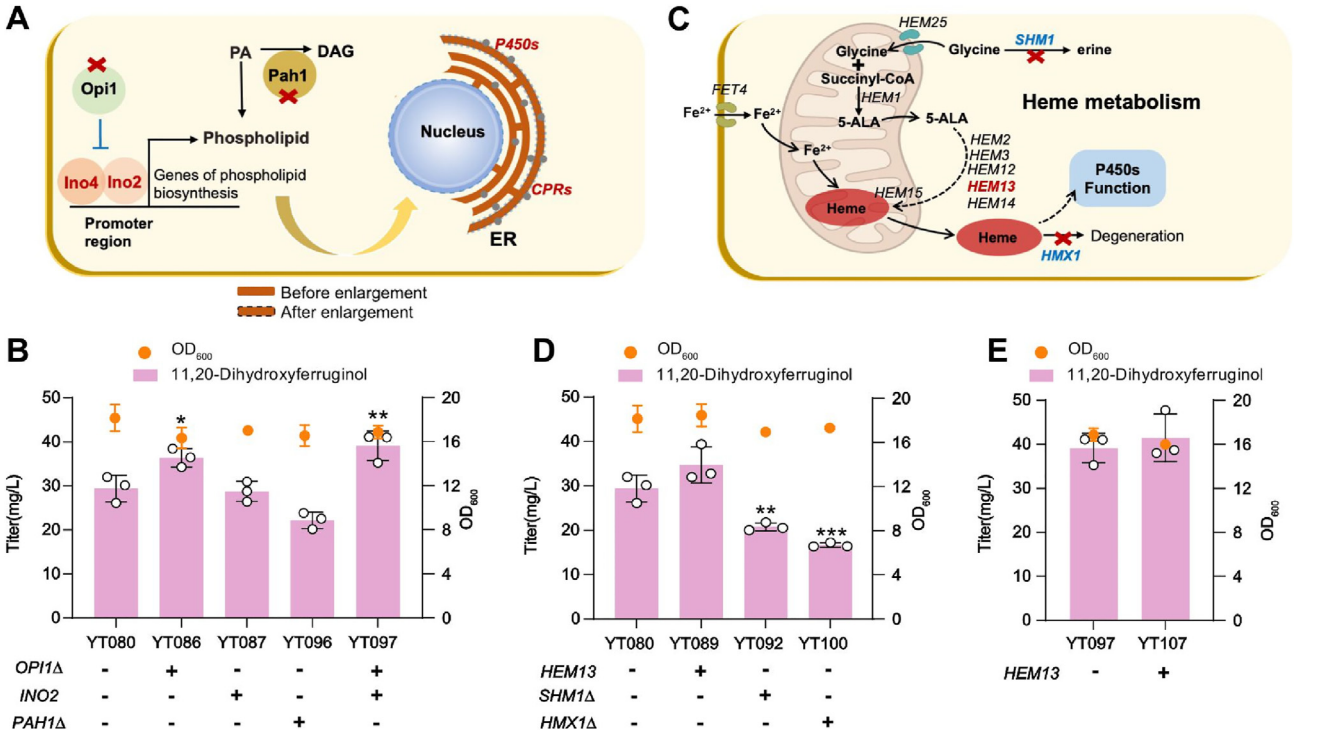

Figure 5 Engineering ER and heme supply to improve 11,20-dihydroxyferruginol biosynthesis. Schematic illustration of genetic modifications resulting from ER engineering (A) and heme engineering (C) to improve the activities of P450s. The blue arrow represents genes that repress a metabolic gene. PA: phosphatidic acid, DAG: diacylglycerol, Ino2 and Ino4: transcriptional activator that binds to a conserved upstream activating sequence (UAS_{INO}) residing in the promoters of phospholipid biosynthetic genes, Opi1: the transcriptional repressor of Ino2 and Ino4 heterodimer, Pah1: PA phosphatase, *HEM1*: 5-aminolevulinate (ALA) synthase gene, *HEM2*: 5-ALA dehydratase gene, *HEM3*: 4-porphobilinogen deaminase gene, *HEM12*: uroporphyrinogen decarboxylase gene, *HEM13*: coproporphyrinogen III oxidase gene, *HEM15*: ferrochelatase gene, *FET4*: low-affinity Fe^{2+} transporter gene, *HEM14*: protoporphyrinogen oxidase gene, *HEM25*: mitochondrial glycine transporter gene, *SHM1*: mitochondrial serine hydroxymethyltransferase gene, *HMX1*: heme oxygenase gene. (B) The titer of 11,20-dihydroxyferruginol is influenced by optimizing the genes to expand ER. (D) The effect of overexpression *HEM13*, deletion of *SHM1*, and *HMX1* genes on the yield of 11,20-dihydroxyferruginol. (E) The yield of 11,20-dihydroxyferruginol after overexpressing *HEM13* of strain YT107. The OD_{600} was measured at the end of fermentation.

low-affinity system is modulated by Yap5p, which activates the expression of specific target genes, including the vacuolar iron importer gene *CCC1*, the Aft1/2p funactional inhibitor genes *GRX3* and *GRX4*[54,55], and *TYW1* gene which regulating intracellular iron content to protect cells from high iron toxicity[56]. Additionally, Yap5p indirectly suppresses and inhibits iron transport gene *FET3*[57]. In response to iron deficiency, *S. cerevisiae* activates the iron regulon *via* two low-iron-sensing transcriptional activators, Aft1p and its paralog Aft2p[53]. These activators induce the expression of a suite of genes, including those encoding components of the reductive iron uptake system (*e.g.*, *FET3, FTR1*, and *FIT2*), as well as mRNA-binding genes *CTH1* and *CTH2* which limit the expression of genes encoding for iron-containing proteins or that participate in iron-using processes[58].

Analysis of the transcriptome data of strain YT011 overexpressed with and without P450s (data not shown in this study) revealed that genes involved in iron-sulfur cluster biosynthesis and iron uptake were upregulated. However, few studies have verified whether engineered iron uptake can enhance the catalytic activity of P450s. Here, we tried to engineer iron uptake and iron-sulfur cluster biosynthesis to increase the catalytic activity of P450s in yeast. These strategies include, (1) enhancing iron uptake from the environment by overexpressing *FIT2*, *FET3*, *FTR1, AFT1*, truncated *TYW1* (*tTYW1*, which could enhance the expression of *AFT1/AFT2*[59]), and deleting *BOL2*, (2) weakening iron competitive pathways by deleting *YAP5*, *GRX3* and *GRX4* and down-regulating *CCC1* expression to reduce iron transport into the vacuole, (3) improving iron-sulfer cluster biosynthesis through overexpressing ISU and CIA machinery genes *NFS1*, *ISU2*, *CFD1*, and *CIA2* (Fig. 6A).

Firstly, the genes related to enhancing iron uptake were engineered. The results showed that overexpression of *FIT2*, *FET3* and *FTR1* led to an increase in the production of 11,20-dihydroxyferruginol to 45.48 ± 13.25 mg/L (strain YT113 in Fig. 6B and Supporting Information Fig. S13). The strain YT113 was further engineered targeting *BOL2* and *tTYW1* to construct stains YT125-YT127. While the most productive strain was YT125, and the production of 11,20-dihydroxyferruginol was 56.63 ± 2.43 mg/L by deleting *BOL2* (Fig. 6C).

Secondly, the deletion of *GRX3* and *GRX4* and the replacement the native promoter of *CCC1* with a weak promoter[60] to increase the intracellular level of iron were employed to engineer in strain YT125. The deletion of *GRX3* and *GRX4* in strain YT125 did not increase the titer of 11,20-dihydroxyferruginol (Supporting Information Fig. S14). Replacing the native promoter of *CCC1* with the *CYB2p* promoter produced an 8% increase in 11,20-dihydroxyferruginol production in strain YT133 (60.98 ± 5.24 mg/L, in Fig. 6D and Supporting Information Table S12).

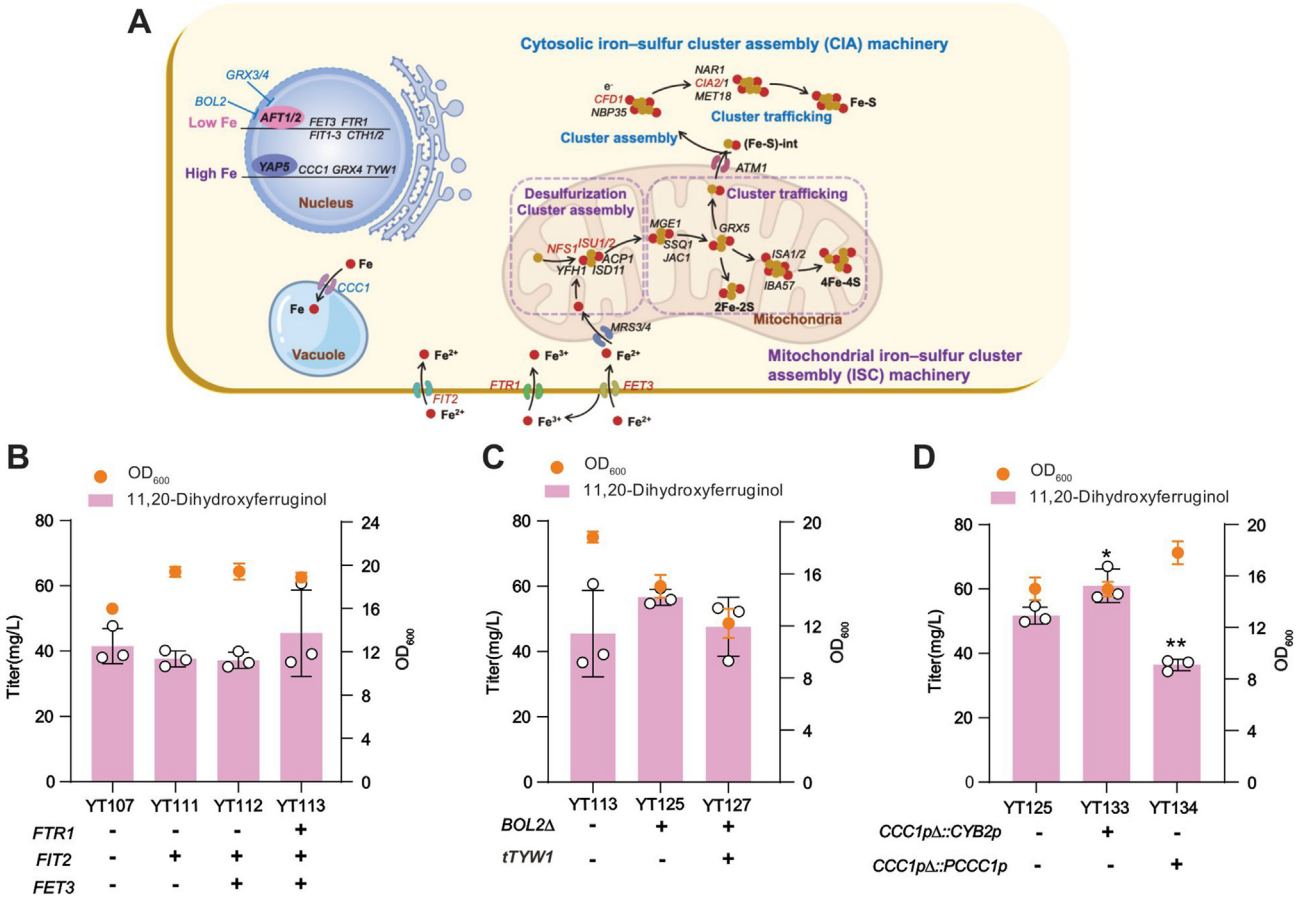

Figure 6 Engineering iron uptake for enhancing the productivity of 11,20-dihydroxyferruginol. (A) Schematic illustration of engineered iron uptake and iron-sulfur cluster metabolism. The red and yellow solid circles represent iron and sulfur, respectively. *FTR1*: high-affinity iron transport gene, *FET3*: high-affinity iron transport gene, *FIT2*: iron siderophore transport gene, *NBP35/CFD1*: cytosolic scaffold−protein complex gene, *MET18/NAR1/CIA1/2*: cytosolic iron-sulfur assembly protein-encoding gene, *CTH1/2*: mRNA-binding genes, *BOL2*: BolA protein gene inhibiting *AFT1/2*, *TYW1*: iron-sulfur cluster enzyme-encoding gene, *YAP5*: iron transcription factor gene, regulating genes in response to excess iron, *GRX3/4*: cytosolic glutaredoxin gene inhibiting *AFT1/2*, *AFT1/2*: iron transcription factor genes coordinating the activation of genes upon iron scarcity, *NFS1*:cysteine desulfurase gene, *ISU1/2*: mitochondrial scaffold protein to assemble [2Fe−2S] cluster gene, *MRS3/4*: iron transporter importing iron into mitochondria gene, *CCC1*: vacuolar iron importer gene, *GRX5*: monothiol glutaredoxin gene, *ATM1*: ABC transporter exporting iron-sulfur intermediates ((Fe−S)-int) from mitochondria to cytoplasm gene, *YFH1*: iron-binding protein frataxin, *JAC1*: J-type chaperone gene, *MGE1/ISA1/2*: iron-sulfur scaffold protein genes involving in maturation of cellular iron-sulfur proteins, *SSQ1*: iron-sulfur cluster assembly protein gene, *IBA57*:mitochondrial iron-sulfur assembly proteins gene. (B) The titer of 11,20-dihydroxyferruginol in engineered strain. (C) The effects on the yield of 11,20-dihydroxyferruginol by deleting *BOL2* and overexpressing *tTYW1* genes. (D) Improving 11,20-dihydroxyferruginol production by replacing the promoter of *CCC1* to downregulate *CCC1* gene expression. And OD_{600} was measured at the end of fermentation.

Lastly, *YAP5*, *GRX3* and *GRX4* were deleted in strain YT133, respectively. Deletion of *YAP5, GRX3* and *GRX4* led to an improvement on the yield of 11,20-dihydroxyferruginol in engineered strain (Table 1). While there was no increase in the production after deleting *GRX3* or *GRX4* in the *YAP5* deleted strain (Supporting Information Fig. S14). Additionally, the overexpression of genes involved in iron-sulfur cluster biosynthesis and *AFT1* did not demonstrate any positive effects on the production of 11,20-dihydroxyferruginol (Fig. S14). Here, the deletion of *YAP5* resulted in the greast improvement of 11,20-dihydroxyferruginol production in strain YT142 which was 67.69 ± 1.33 mg/L in shake flasks (Table 1 and Supporting Information Fig. S15). However, further systematic investigation regarding the coordination of different genes remains necessary (Supporting Information Figs. S16 and S17).

Table 1 The titers of 11,20-dihydroxyferruginol in deleting *GRX3*, *GRX4*, and *YAP5* genes in engineered strains.

Stain	Genotype	Titer (mg/L)
YT139	YT133, *GRX3Δ*	65.45 ± 2.40
YT141	YT133, *GRX4Δ*	65.90 ± 1.42
YT142	YT133, *YAP5Δ*	67.69 ± 1.33

4. Conclusions

P450s represent one of the largest and most diverse protein superfamilies known for catalyzing a broad spectrum of regiospecific, stereospecific, and irreversible reactions within the biosynthetic pathways of various pharmacologically active PNPs

used in human therapeutics. Moreover, P450s act as crucial rate-limiting factors in both PNP biosynthesis and synthetic biology approaches for PNP production. In this study, to enhance the catalytic activity of P450s in *S. cerevisiae*, we adopted effective strategies to optimize the overall catalytic microenvironment of three P450s involved in the biosynthesis of 11,20-dihydroxyferruginol, the precursor of tanshinones. By enhancing MVA pathway, coexpressing with redox partner genes, overexpressing *TRP1*, *LEU2*, and *LYS2* genes, deleting *GAL80*, engineering NADPH and heme supply, expanding the ER, and regulating iron uptake, we achieved a remarkable 42.1-fold improvement in 11,20-dihydroxyferruginol titer compared to that of the starting strain YT009. Our findings demonstrated that regulat iron uptake could promote the active expression of P450s and lead to improving their catalytic activity. Overall, this study makes progress in the development of synthetic yeast cell factories harboring multiple P450s and paves the way for microbial biosynthesis of tanshinones.

Acknowledgments

This work was supported by the National Key R&D Program of China (2020YFA0908000), Scientific and technological innovation project of China Academy of Chinese Medical Sciences (CI2023D002, CI2023E002, CI2021A04110, CI2021B014), the National Natural Science Foundation of China (81822046), Key project at central government level: The ability to establish sustainable use of valuable Chinese medicine resources (2060302). The authors thank Professor Yongjin Zhou for the kind gifts of plasmids pECAS9-gRNA-KanMX-tHFD and pgRNA-KanMX.

Author contributions

Yatian Cheng: Writing − original draft, Methodology, Investigation, Formal analysis, Data curation, Conceptualization. Linglong Luo: Resources, Formal analysis. Hao Tang: Resources, Formal analysis. Jian Wang: Methodology, Formal analysis. Li Ren: Resources, Formal analysis. Guanghong Cui: Formal analysis. Yujun Zhao: Formal analysis. Jinfu Tang: Methodology, Data curation. Ping Su: Methodology, Formal analysis. Yanan Wang: Methodology, Formal analysis. Yating Hu: Methodology, Formal analysis. Ying Ma: Writing − review & editing, Software, Resources, Methodology, Funding acquisition, Formal analysis, Data curation, Conceptualization. Juan Guo: Writing − review & editing, Validation, Resources, Project administration, Methodology, Investigation, Funding acquisition, Formal analysis, Conceptualization. Luqi Huang: Project administration, Funding acquisition.

Conflicts of interest

The authors declare no conflicts of interest.

Appendix A. Supporting information

Supporting information to this article can be found online at https://doi.org/10.1016/j.apsb.2024.05.019.

References

1. Parvez M, Qhanya LB, Mthakathi NT, Kgosiemang IK, Bamal HD, Pagadala NS, et al. Molecular evolutionary dynamics of cytochrome P450 monooxygenases across kingdoms: special focus on mycobacterial P450s. *Sci Rep* 2016;**6**:33099.
2. Elfaki I, Mir R, Almutairi FM, Duhier FMA. Cytochrome P450: polymorphisms and roles in cancer, diabetes and atherosclerosis. *Asian Pac J Cancer Prev* 2018;**19**:2057−70.
3. Nelson DR. Cytochrome P450 diversity in the tree of life. *Biochim Biophys Acta Proteins Proteom* 2018;**1866**:141−54.
4. Alzahrani AM, Rajendran P. The multifarious link between cytochrome P450s and cancer. *Oxid Med Cell Longev* 2020;**2020**:3028387.
5. Yu AM, Zhong XB. Advanced knowledge in drug metabolism and pharmacokinetics. *Acta Pharm Sin B* 2016;**6**:361−2.
6. Hammer SC, Kubik G, Watkins E, Huang S, Minges H, Arnold FH. Anti-markovnikov alkene oxidation by metal-oxo-mediated enzyme catalysis. *Science* 2017;**358**:215−8.
7. Ma Y, Cai Y, Ma X, Cui G, Tang J, Zen W, et al. Research progress of P450 in the biosynthesis of bioactive compound of medicinal plants. *Acta Pharma Sin* 2020;**55**:1573−89.
8. Hamberger B, Bak S. Plant P450s as versatile drivers for evolution of species-specific chemical diversity. *Philos Trans R Soc Lond B Biol Sci* 2013;**368**:20120426.
9. Renault H, Bassard JE, Hamberger B, Werck-Reichhart D. Cytochrome P450-mediated metabolic engineering: current progress and future challenges. *Curr Opin Plant Biol* 2014;**19**:27−34.
10. Liu X, Luo L, Ma Y, Bu J, Hu Z, Sun S, et al. Biopathway construction of plant natural products. *Acta Pharma Sin* 2021;**56**:3285−99.
11. Jiang B, Gao L, Wang H, Sun Y, Zhang X, Ke H, et al. Characterization and heterologous reconstitution of Taxus biosynthetic enzymes leading to baccatin III. *Science* 2024;**383**:622−9.
12. Zhang J, Hansen LG, Gudich O, Viehrig K, Lassen LMM, Schrübbers L, et al. A microbial supply chain for production of the anti-cancer drug vinblastine. *Nature* 2022;**609**:341−7.
13. Liu Q, Liu Y, Li G, Savolainen O, Chen Y, Nielsen J. *De novo* biosynthesis of bioactive isoflavonoids by engineered yeast cell factories. *Nat Commun* 2021;**12**:6085.
14. Zhao F, Bai P, Liu T, Li D, Zhang X, Lu W, et al. Optimization of a cytochrome P450 oxidation system for enhancing protopanaxadiol production in *Saccharomyces cerevisiae*. *Biotechnol Bioeng* 2016;**113**:1787−95.
15. Tu L, Cai X, Zhang Y, Tong Y, Wang J, Su P, et al. Mechanistic analysis for the origin of diverse diterpenes in *Tripterygium wilfordii*. *Acta Pharm Sin B* 2022;**12**:2923−33.
16. Zhang Y, Gao J, Ma L, Tu L, Hu T, Wu X, et al. Tandemly duplicated CYP82Ds catalyze 14-hydroxylation in triptolide biosynthesis and precursor production in *Saccharomyces cerevisiae*. *Nat Commun* 2023;**14**:875.
17. Li Z, Jiang Y, Guengerich FP, Ma L, Li S, Zhang W. Engineering cytochrome P450 enzyme systems for biomedical and biotechnological applications. *J Biol Chem* 2020;**295**:833−49.
18. Jensen K, Møller BL. Plant NADPH-cytochrome P450 oxidoreductases. *Phytochemistry* 2010;**71**:132−41.
19. Durairaj P, Hur JS, Yun H. Versatile biocatalysis of fungal cytochrome P450 monooxygenases. *Microb Cell Fact* 2016;**15**:125.
20. Zhang X, Guo J, Cheng F, Li S. Cytochrome P450 enzymes in fungal natural product biosynthesis. *Nat Prod Rep* 2021;**38**:1072−99.
21. Jiang Z, Gao W, Huang L. Tanshinones, critical pharmacological components in *Salvia miltiorrhiza*. *Front Pharmacol* 2019;**10**:202.
22. Cheng Y, Tang H, Sun L, Hu Y, Ma Y, Guo J, et al. Advances on the microbial synthesis of plant-derived diterpenoids. *Sheng Wu Gong Cheng Xue Bao* 2023;**39**:2265−83.
23. Zhang Y, Xu Z, Ji A, Luo H, Song J. Genomic survey of bZIP transcription factor genes related to tanshinone biosynthesis in *Salvia miltiorrhiza*. *Acta Pharm Sin B* 2018;**8**:295−305.

24. Guo J, Ma X, Cai Y, Ma Y, Zhan Z, Zhou YJ, et al. Cytochrome P450 promiscuity leads to a bifurcating biosynthetic pathway for tanshinones. *New Phytol* 2016;**210**:525−34.
25. Guo J, Zhou YJ, Hillwig ML, Shen Y, Yang L, Wang Y, et al. CYP76AH1 catalyzes turnover of miltiradiene in tanshinones biosynthesis and enables heterologous production of ferruginol in yeasts. *Proc Natl Acad Sci U S A* 2013;**110**:12108−13.
26. Zhou YJ, Gao W, Rong Q, Jin G, Chu H, Liu W, et al. Modular pathway engineering of diterpenoid synthases and the mevalonic acid pathway for miltiradiene production. *J Am Chem Soc* 2012;**134**:3234−41.
27. Hu T, Zhou J, Tong Y, Su P, Li X, Liu Y, et al. Engineering chimeric diterpene synthases and isoprenoid biosynthetic pathways enables high-level production of miltiradiene in yeast. *Metab Eng* 2020;**60**:87−96.
28. Zhu Z, Zhou YJ, Kang MK, Krivoruchko A, Buijs NA, Nielsen J. Enabling the synthesis of medium chain alkanes and 1-alkenes in yeast. *Metab Eng* 2017;**44**:81−8.
29. Funes Chaban M, Hrast M, Frlan R, Graikioti DG, Athanassopoulos CM, Carpinella MC. Inhibition of MurA enzyme from *Escherichia coli* and *Staphylococcus aureus* by diterpenes from *Lepechinia meyenii* and Their synthetic analogs. *Antibiotics (Basel)* 2021;**10**:1535.
30. Mans R, van Rossum HM, Wijsman M, Backx A, Kuijpers NG, van den Broek M, et al. CRISPR/Cas9: a molecular Swiss army knife for simultaneous introduction of multiple genetic modifications in *Saccharomyces cerevisiae*. *FEMS Yeast Res* 2015;**15**:fov004.
31. Jessop-Fabre MM, Jakociunas T, Stovicek V, Dai Z, Jensen MK, Keasling JD, et al. EasyClone-MarkerFree: a vector toolkit for marker-less integration of genes into *Saccharomyces cerevisiae via* CRISPR-Cas9. *Biotechnol J* 2016;**11**:1110−7.
32. Chen R, Gao J, Yu W, Chen X, Zhai X, Chen Y, et al. Engineering cofactor supply and recycling to drive phenolic acid biosynthesis in yeast. *Nat Chem Biol* 2022;**18**:520−9.
33. Liu T, Gou Y, Zhang B, Gao R, Dong C, Qi M, et al. Construction of ajmalicine and sanguinarine de novo biosynthetic pathways using stable integration sites in yeast. *Biotechnol Bioeng* 2022;**119**:1314−26.
34. Gietz RD, Woods RA. Transformation of yeast by lithium acetate/single-stranded carrier DNA/polyethylene glycol method. *Methods Enzymol* 2002;**350**:87−96.
35. Sinha T, Makia M, Du J, Naash MI, Al-Ubaidi MR. Flavin homeostasis in the mouse retina during aging and degeneration. *J Nutr Biochem* 2018;**62**:123−33.
36. Michener JK, Nielsen J, Smolke CD. Identification and treatment of heme depletion attributed to overexpression of a lineage of evolved P450 monooxygenases. *Proc Natl Acad Sci U S A* 2012;**109**:19504−9.
37. Ishchuk OP, Domenzain I, Sanchez BJ, Muniz-Paredes F, Martinez JL, Nielsen J, et al. Genome-scale modeling drives 70-fold improvement of intracellular heme production in *Saccharomyces cerevisiae*. *Proc Natl Acad Sci U S A* 2022;**119**:e2108245119.
38. Yang S, Cao X, Yu W, Li S, Zhou YJ. Efficient targeted mutation of genomic essential genes in yeast *Saccharomyces cerevisiae*. *Appl Microbiol Biotechnol* 2020;**104**:3037−47.
39. Perez-Gonzalez A, Kniewel R, Veldhuizen M, Verma HK, Navarro-Rodriguez M, Rubio LM, et al. Adaptation of the GoldenBraid modular cloning system and creation of a toolkit for the expression of heterologous proteins in yeast mitochondria. *BMC Biotechnol* 2017;**17**:80.
40. Muzaffar S, Chattoo BB. Apoptosis-inducing factor (Aif1) mediates anacardic acid-induced apoptosis in *Saccharomyces cerevisiae*. *Apoptosis* 2017;**22**:463−74.
41. Chin C, Donaghey F, Helming K, McCarthy M, Rogers S, Austriaco N. Deletion of *AIF1* but not of *YCA1/MCA1* protects *Saccharomyces cerevisiae* and *Candida albicans* cells from caspofungin-induced programmed cell death. *Microb Cell* 2014;**1**:58−63.
42. Ignea C, Trikka FA, Nikolaidis AK, Georgantea P, Ioannou E, Loupassaki S, et al. Efficient diterpene production in yeast by engineering Erg20p into a geranylgeranyl diphosphate synthase. *Metab Eng* 2015;**27**:65−75.
43. Schulz V, Freibert SA, Boss L, Mühlenhoff U, Stehling O, Lill R. Mitochondrial [2Fe−2S] ferredoxins: new functions for old dogs. *FEBS Lett* 2023;**597**:102−21.
44. Kim JE, Jang IS, Sung BH, Kim SC, Lee JY. Rerouting of NADPH synthetic pathways for increased protopanaxadiol production in *Saccharomyces cerevisiae*. *Sci Rep* 2018;**8**:15820.
45. Shi Y, Dong T, Zeng B, Yao M, Wang Y, Xie Z, et al. Production of plant sesquiterpene lactone parthenolide in the yeast cell factory. *ACS Synth Biol* 2022;**11**:2473−83.
46. Kwak S, Yun EJ, Lane S, Oh EJ, Kim KH, Jin YS. Redirection of the glycolytic flux enhances isoprenoid production in *Saccharomyces cerevisiae*. *Biotechnol J* 2020;**15**:e1900173.
47. Kim JE, Jang IS, Son SH, Ko YJ, Cho BK, Kim SC, et al. Tailoring the *Saccharomyces cerevisiae* endoplasmic reticulum for functional assembly of terpene synthesis pathway. *Metab Eng* 2019;**56**:50−9.
48. Schuck S, Prinz WA, Thorn KS, Voss C, Walter P. Membrane expansion alleviates endoplasmic reticulum stress independently of the unfolded protein response. *J Cell Biol* 2009;**187**:525−36.
49. Adeyo O, Horn PJ, Lee S, Binns DD, Chandrahas A, Chapman KD, et al. The yeast lipin orthologue Pah1p is important for biogenesis of lipid droplets. *J Cell Biol* 2011;**192**:1043−55.
50. Biz A, Mahadevan R. Overcoming challenges in expressing iron-sulfur enzymes in yeast. *Trends Biotechnol* 2021;**39**:665−77.
51. Bamba T, Yukawa T, Guirimand G, Inokuma K, Sasaki K, Hasunuma T, et al. Production of 1,2,4-butanetriol from xylose by *Saccharomyces cerevisiae* through Fe metabolic engineering. *Metab Eng* 2019;**56**:17−27.
52. Li L, Ward DM. Iron toxicity in yeast: transcriptional regulation of the vacuolar iron importer Ccc1. *Curr Genet* 2018;**64**:413−6.
53. Martins TS, Costa V, Pereira C. Signaling pathways governing iron homeostasis in budding yeast. *Mol Microbiol* 2018;**109**:422−32.
54. Pimentel C, Vicente C, Menezes RA, Caetano S, Carreto L, Rodrigues-Pousada C. The role of the Yap5 transcription factor in remodeling gene expression in response to Fe bioavailability. *PLoS One* 2012;**7**:e37434.
55. Gibson LM, Dingra NN, Outten CE, Lebioda L. Structure of the thioredoxin-like domain of yeast glutaredoxin 3. *Acta Crystallogr D Biol Crystallogr* 2008;**64**:927−32.
56. Li L, Miao R, Bertram S, Jia X, Ward DM, Kaplan J. A role for iron-sulfur clusters in the regulation of transcription factor Yap5-dependent high iron transcriptional responses in yeast. *J Biol Chem* 2012;**287**:35709−21.
57. Martinez-Pastor MT, Perea-Garcia A, Puig S. Mechanisms of iron sensing and regulation in the yeast *Saccharomyces cerevisiae*. *World J Microbiol Biotechnol* 2017;**33**:75.
58. Ramos-Alonso L, Romero AM, Martinez-Pastor MT, Puig S. Iron regulatory mechanisms in *Saccharomyces cerevisiae*. *Front Microbiol* 2020;**11**:582830.
59. Li L, Jia X, Ward DM, Kaplan J. Yap5 protein-regulated transcription of the *TYW1* gene protects yeast from high iron toxicity. *J Biol Chem* 2011;**286**:38488−97.
60. Yu T, Zhou YJ, Huang M, Liu Q, Pereira R, David F, et al. Reprogramming yeast metabolism from alcoholic fermentation to lipogenesis. *Cell* 2018;**174**:1549. 58.e14.